Assessment of the three-dimensional flow field in the reactor pressure vessel in Hualong One nuclear power plants

Zonglan Wei, Songwei Li*, Sijia Du, Yazhe Lu and Zhifang Qiu

Science and Technology on Reactor System Design Technology Laboratory, Nuclear Power Institute of China, Chengdu, Sichuan, China

This study uses computational fluid dynamics (CFD) to investigate the three-dimensional flow field under normal operating conditions in the reactor pressure vessel (RPV) in the Hualong One nuclear power plants (NPPs). With a particular focus on the flowrate distribution at the core inlet, the numerical framework is validated against the integral hydraulic experiment in a 1:4-scaled RPV of CNP1000, the prototype of the Hualong One reactor. The simulation results of the normalized flowrate at the core inlet agree reasonably well with the measured data. Based on the experimental data, several methods of calibrating the CFD turbulence model coefficients are suggested by introducing the concepts of data assimilation and machine learning. The flow field in a realistic RPV for Hualong One is predicted using the validated numerical framework, showing that the flowrate distribution at the core inlet is nearly homogeneous and that the turbulent intensity is acceptably low for each fuel assembly. It can provide essential information for the reactor core thermal–hydraulic design and the fuel assembly mechanical assessment.

KEYWORDS

computational fluid dynamics, reactor pressure vessel, flowrate distribution, data assimilation, turbulence model

1 Introduction

The reactor pressure vessel (RPV) is a key component of a nuclear power plant. Normally, the RPV consists of more than 1000 complex structural parts, including the internal components in the upper and lower plenum and the reactor core with fuel assemblies. Generally, the flow circulation in the RPV is established through the cold legs, downcomer (DC), lower plenum (LP), reactor core, upper plenum (UP), and, eventually, the hot legs. Due to the geometric complexity along the whole circulation path in the RPV and the high velocity of the coolant under normal operation conditions, the coolant flow is highly turbulent with three-dimensional irregularity, which can be characterized by unstable eddies in a broad range of spatial and temporal scales. Nevertheless, some special internal components in the lower plenum are designed to function as flow straighteners to ensure that the flowrate for each fuel assembly at the core inlet is approximately the same. This is because the homogeneous coolant flow distribution at the core inlet is a demanding feature for the reactor's thermal–hydraulic and mechanical design. Therefore, a comprehensive understanding and accurate predictions of the three-dimensional flow field in the RPV are crucially important.

FIGURE 1
Mock-up RPV of the CNP1000 experiment.

The Hualong One nuclear power plant (NPP), an internationally recognized type of third-generation NPP, was independently designed and developed by the Nuclear Power Institute of China (NPIC). At the beginning of the Hualong One research and development period, a prototype named CNP1000 was designed. Based on a 1:4-scaled experimental facility of the CNP1000 RPV, integral hydraulic experiments were conducted and the flowrate distribution at the core inlet was measured. The scaled vessel retains the major internal structures in the CNP 1000 RPV. The fuel assemblies in the reactor core are simplified with a bundle of aluminum tubes, the so-called "core simulator," to attain appropriate hydraulic resistance that does not significantly influence the velocity field in the DC and LP of the vessel. The flowrate in the experimental circuit is determined according to the flow similarity criterion in order to obtain the normalized flowrate distribution at the core inlet under the normal operation conditions of the reactor. The present Hualong One RPV shares overall structural similarity with the CNP1000 RPV, while many local components, especially in the LP, have been optimized. No more integral hydraulic tests are being performed to investigate the flowrate distribution at the core inlet, but, with the aid of computational fluid dynamics (CFD), numerical simulations can be conducted to assess the three-dimensional flow field in the RPV. It has been demonstrated by academic research and industrial practice that, with the properly validated numerical framework,

CFD can obtain relatively accurate key flow parameters compared to experimental measurement by consuming less time and resources (Ferziger and Peric, 2001).

Since the 1990s, CFD has become popular in nuclear engineering, and it is used for the quantitative assessment of the flow field in the fuel assembly, turbulent mixing in the LP and UP, pressurized thermal shock on structural components, and hydrogen distribution in the containment. Frepoli (1996) simulated the turbulent flow field in a simplified boiling water reactor using the code FLOW3D. Gango (1997) analyzed the boron dilution process in the LP of the Loviisa NPP, a VVER-440 type, using the code PHOENICS. The No. 43 OECD/CSNI international benchmark was established for numerical code verification based on the rapid boron-dilution transient tests performed by the University of Maryland (Gavrilas and Kiger, 2000). Ten participants from eight countries have submitted their results using various codes, including commercial codes like ANSYS CFX and ANSYS FLUENT and in-house codes like PLASHY and TRIO_U. Most of the numerical results could match the experimental data quite well, implying that CFD codes are capable of predicting the complex flow field in the reactor. In the framework of the FLOMIX-R project (Rohde et al., 2005), many essential nuclear reactor thermal hydraulic safety issues relevant to pressurized water reactor (PWR) NPPs have been systematically investigated by experimental testing and numerical simulations. The experimental facilities include the ROCOM facility, a scaled model of a German KONVOI-type PWR, the VATTENFALL facility, a scaled model of a Westinghouse three-loop PWR, and the EDO Gidropress facility, a scaled model of a VVER-1000 type PWR. There has been much research into the applicability of CFD methods for numerical simulations of the flow field in the reactor (Glover et al., 2007; Höhne et al., 2007; Rohde et al., 2007; Schaffrath et al., 2007). Bieder et al. (2007) predicted the turbulent mixing in the VVER-1000 RPV downcomer using the in-house code TRIO_U developed by CEA. Wei et al. (Zonglan et al., 2022) used OpenFOAM and the URANS methodology to investigate buoyancy-influenced flows in the RPV under main steam line break accident scenarios and showed that the anisotropic turbulent heat flux models can improve the accuracy of the temperature predictions. The outcomes of the numerical assessment studies have demonstrated that CFD is a reliable tool for the analysis of the flow field in the RPV under most conditions. Consequently, CFD is widely used in the design of third-generation NPPs such as AP1000, EPR, and Hualong One.

The present study discusses the numerical framework for the Hualong One RPV three-dimensional flow field simulation with a particular focus on the coolant flowrate distribution at the core inlet.

2 Methodology

2.1 Geometrical simplification

Based on the three-dimensional geometry of the realistic RPV, the fluid domain was generated after some necessary simplification of the RPV geometry. The sharp chamfers, assembly gaps, and surface holes were simplified because these structures were assumed to be irrelevant to the flow patterns, so ignoring them would significantly improve the quality of the spatial discretization of the fluid domain and the robustness of the simulations.
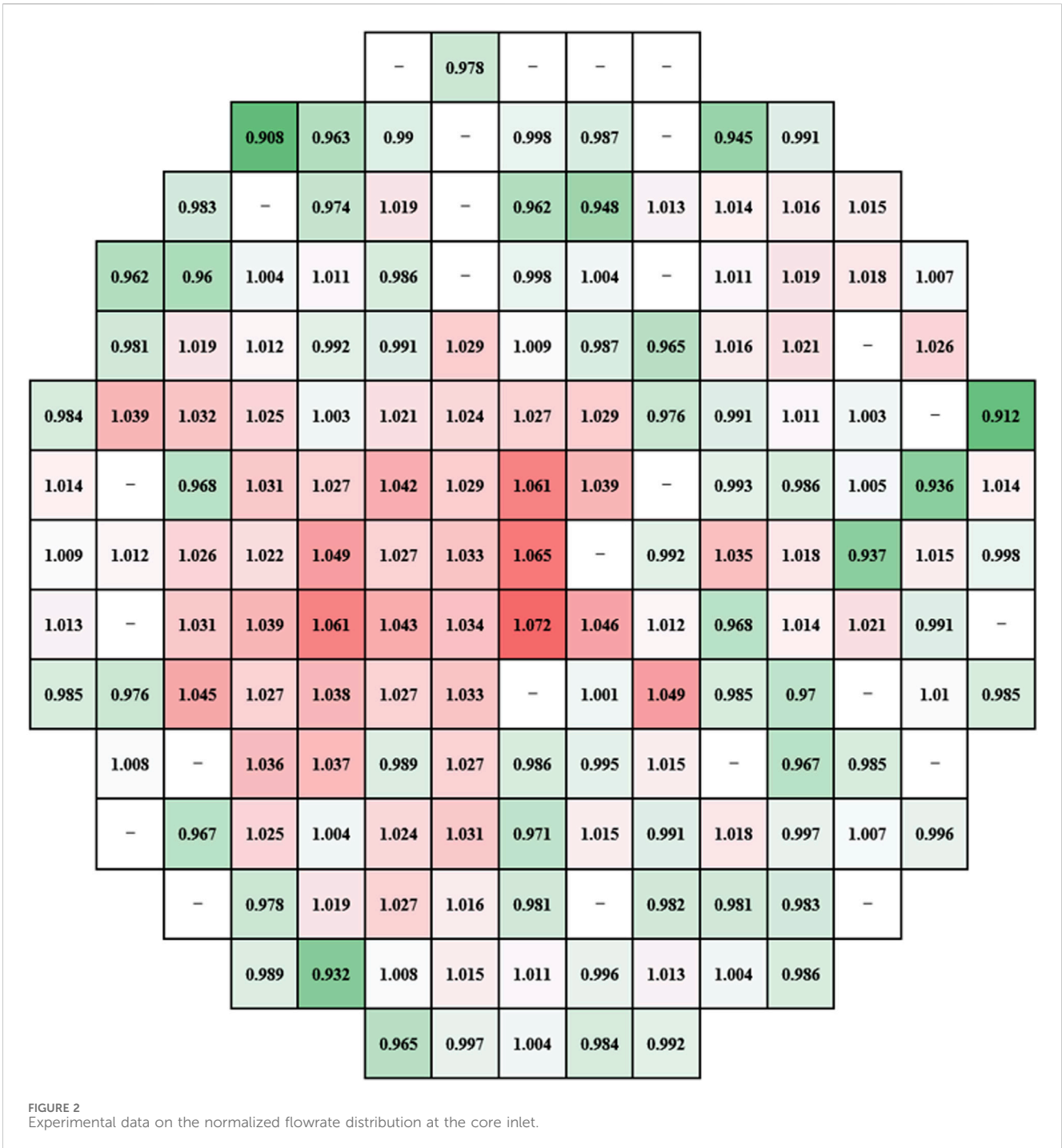
FIGURE 2
Experimental data on the normalized flowrate distribution at the core inlet.

A particular kind of simplification was applied to the reactor core consisting of hundreds of fuel assemblies. The numerical expense would be extreme if all details in the reactor core were considered in the simulations. Considering that the main focus of the numerical study is the flowrate distribution at the core inlet and that the reactor core locates the concerned position downstream, the major role played by the reactor core in the flowrate distribution at the core inlet was the flow resistance boundary. Therefore, the reactor core could be simplified by a polygonal channel shaped by the core barrel with additional momentum source, matching the same pressure drop in the realistic core.

Eventually, the fluid domain was composed of the main structures of the RPV, including the cold legs, DC, LP with supporting components, lower core plate, and a simplified reactor core region.

2.2 Physical model

The Reynolds-averaged Navier–Stokes (RANS) simulation method is the most popular approach for general CFD simulations for practical industrial turbulent flows. Simulations with RANS are normally fast and computationally inexpensive because only the
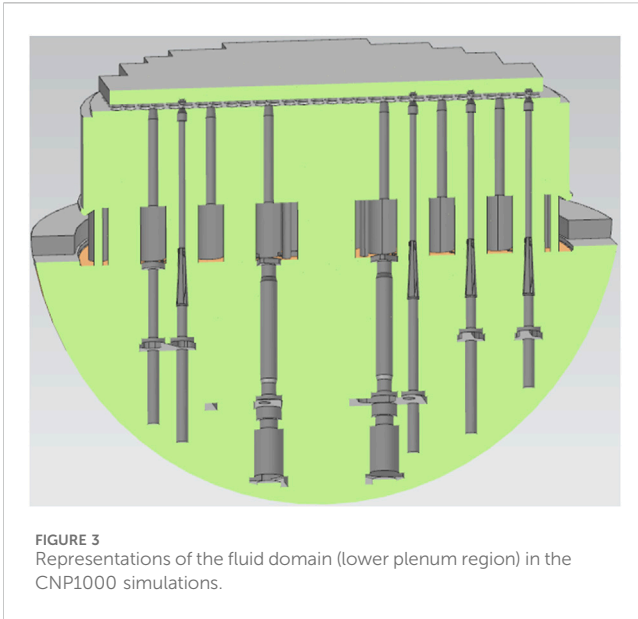
FIGURE 3
Representations of the fluid domain (lower plenum region) in the
CNP1000 simulations.

FIGURE 4
Representations of the fluid domain (core region) in the
CNP1000 simulations.

averaged flow fields are computed by solving the Reynolds-averaged
conservation equations, which bring closure to problems for modeling
unknown terms such as Reynolds stress appearing in the Reynolds-
averaged momentum equation. The Reynolds-averaged governing
equations for incompressible flow can be written as Eqs 1, 2:

$$\frac{\partial \langle U_i \rangle}{\partial x_i} = 0, \tag{1}$$

$$\frac{\partial \langle U_i \rangle}{\partial t} + \frac{\partial \langle U_i \rangle \langle U_j \rangle}{\partial x_j} = -\frac{1}{\rho}\frac{\partial \langle P \rangle}{\partial x_i} + \frac{\partial}{\partial x_j}\left(\nu\left(\frac{\partial \langle U_i \rangle}{\partial x_j} + \frac{\partial \langle U_j \rangle}{\partial x_i}\right)\right)$$
$$-\frac{\partial \langle u_i u_j \rangle}{\partial x_j}, \tag{2}$$

where $\langle U_i \rangle$ and $\langle P \rangle$ are the Reynolds-averaged velocity vector and
pressure, respectively. The constant fluid physical properties are
denoted as ρ for density and ν for kinematic viscosity. The symbol t
is time, and x_i represents the spatial coordinates.

The assumptions for closure of the Reynolds stress $\langle u_i u_j \rangle$ are the
so-called "turbulence models". There are very many turbulence
modeling approaches in the literature, and these models have
different complexity and also vary considerably in computational
cost (Pope, 2000; Moukalled et al., 2016). Nowadays the $k - \varepsilon$ model
(Launder and Sharma, 1974), $k - \omega$ model (Wilcox, 1993), and their
variants (Lien et al., 1996; Menter et al., 2003) are the commonly used
turbulence models in routine industrial applications with RANS
simulations. According to design experience from the Hualong
One research and development, the SST k-ω model (Menter et al.,
2003), which possesses the general advantages of simulating the flow
separation and vortex detachment/reattachment, was selected for the
RPV flow field simulation in the present study.

2.3 Numerical setup

The fluid domain is discretized using tetrahedral cells. The
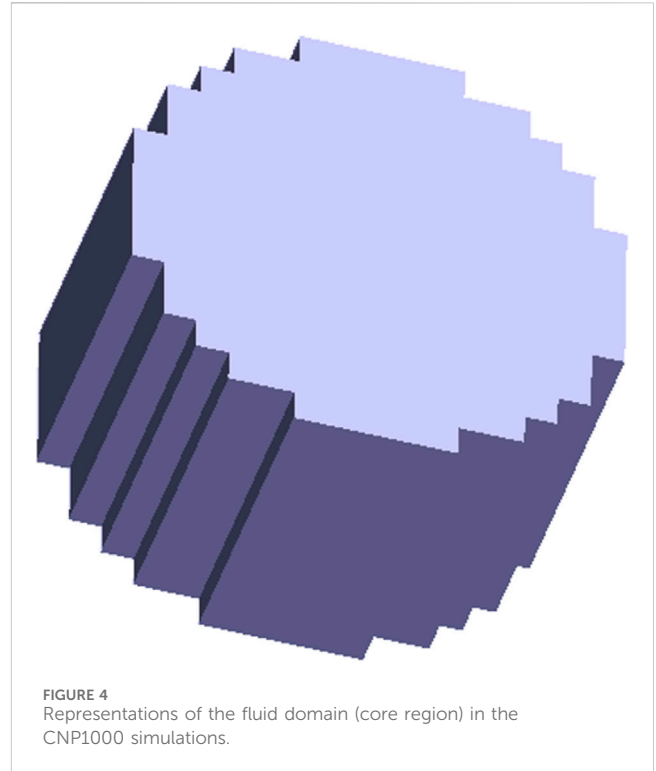spatial discretization schemes are second-order for the advective

terms. The semi-implicit pressure-linked equations (SIMPLE)
algorithm is employed together with the algebraic multi-grid
method to solve the linear system of the discretized equations.

The fixed volumetric flow rates are imposed at the inlets of each
loop, and the adequate length of the CLs ensures that the flow
becomes fully turbulent before entering the DC. The no-slip
boundary condition is imposed at all the walls for velocity, and the
zero-gradient condition is applied for pressure. At the outlet of the
core region, uniform fixed relative static pressure is applied, and the
zero-gradient boundary condition is used for the other quantities. The
directional loss model is particularly used to model the momentum
loss in the reactor core region. A certain resistance loss corresponding
to the pressure drop in the fuel assemblies is achieved in the
streamwise direction in the core region with flow inhibited in the
transverse directions, which is regarded as the equivalent resistance
boundary downstream from the core inlet.

3 Results and discussion

3.1 Simulation results for CNP1000

As the prototype of Hualong One, the CNP1000 RPV shares
overall structural similarities with the Hualong One RPV. Based on
the CNP1000 RPV, integral hydraulic experiments were conducted
in the 1:4 scaled experimental facility (Figure 1). A total of 177 fuel
assembly simulators were placed in sequence in the vessel so that the
resistant characteristics of the reactor core could be reproduced.
Each fuel assembly simulator was equipped with a flowmeter in the
inlet section, thus reflecting the flow distribution at the core inlet
according to the normalized flowrate measurement of all the fuel
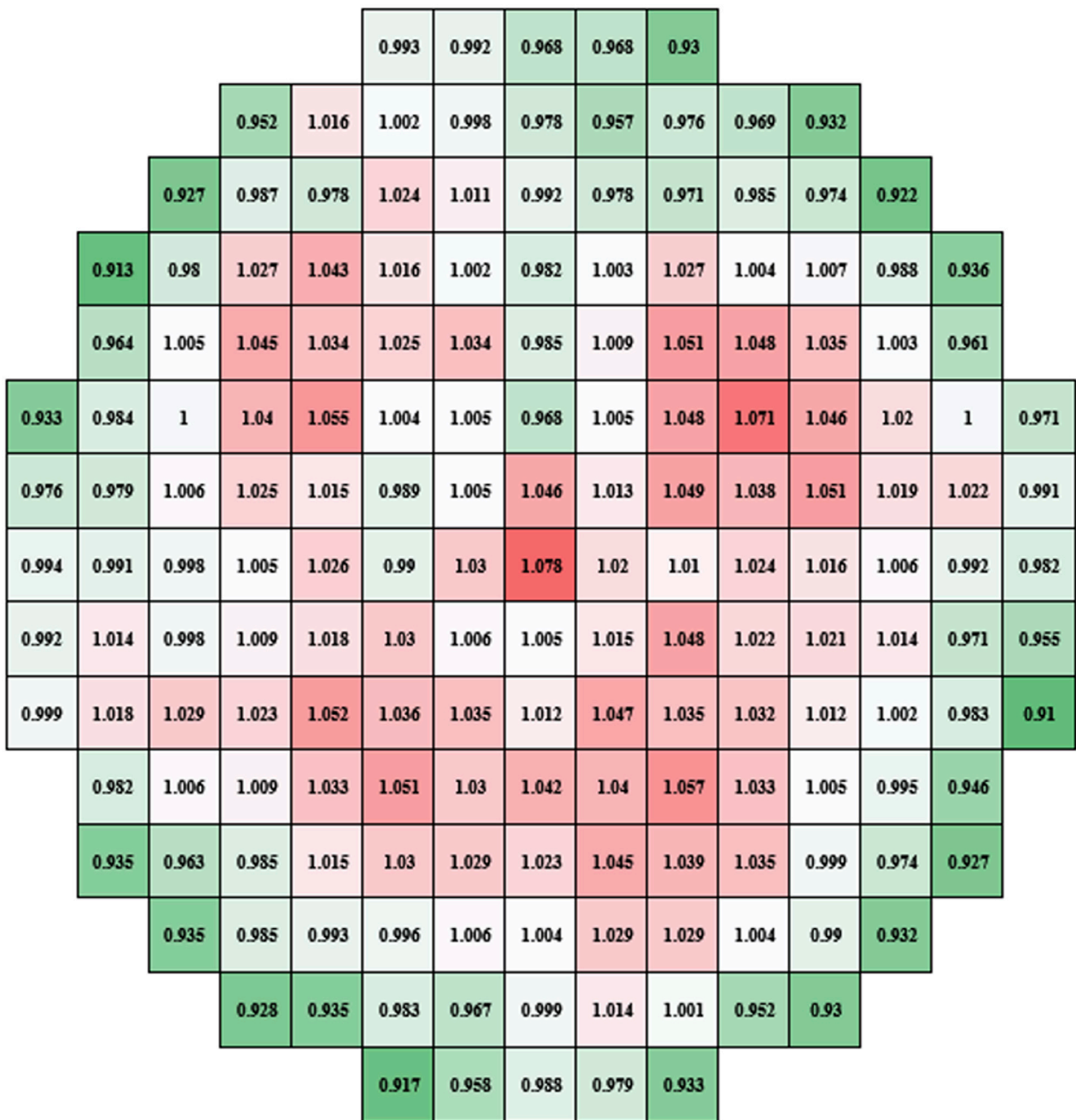assembly simulators. The tests were performed at room temperature

FIGURE 5
Distribution of the normalized flowrate at the core inlet of the CNP1000 simulation.

and atmospheric pressure. The Reynolds number in the core simulator was ensured at over 1.2×10^5, and the total flowrate in the experimental circuit was determined according to the flow similarity criterion. The flowrate for each fuel assembly simulator was recorded by the embedded flowmeter, and the normalized flowrate is defined as Eq. 3:

$$\eta_i = q_i \bigg/ \frac{1}{n} \sum q_i, \qquad (3)$$

where n represents the number of fuel assemblies and q_i is the measured flowrate for the i-th fuel assembly. Only 151 flowmeters

worked normally in the experiments, with the other 26 failing due to layout problems. The measurements were repeated five times for the selected test to minimize the noise not relevant to the flow distribution. The ensemble-averaged data on the normalized flowrate measurement are shown in Figure 2. The distribution of the normalized flowrate is generally quite homogenous, with the highest normalized flowrate (1.07) in the internal fuel assemblies and lowest normalized flowrate (0.91) in the corner fuel assemblies. The major source of experiment data uncertainty was the flowmeter measurement, which is about 0.5%, and the experimental data are suitable for the CFD comparison and further analysis.

FIGURE 6
Profile of the velocity vectors in the lower plenum.
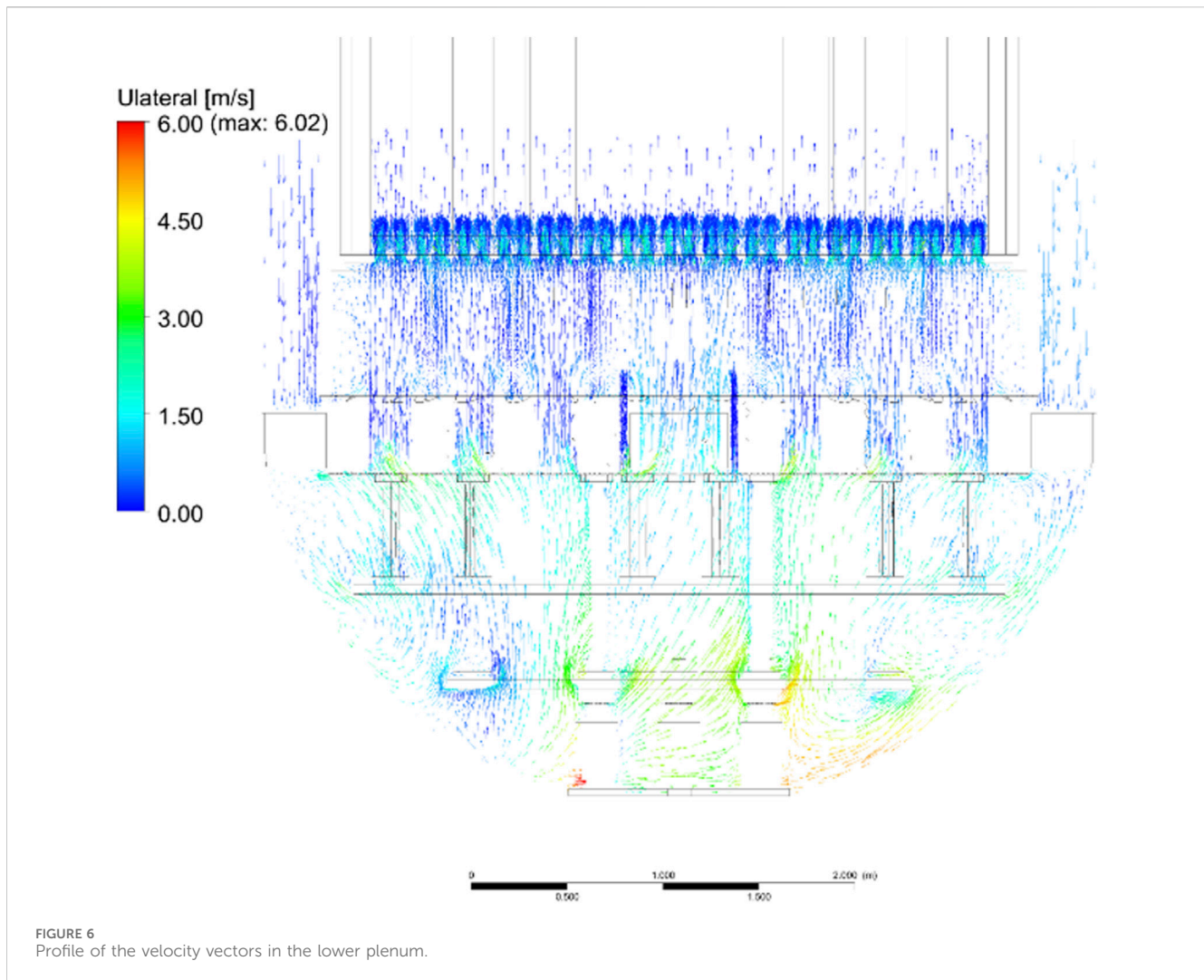
Based on the geometrical simplification and numerical settings discussed in Section 2, the fluid domain for the CFD simulation of the CNP1000 experimental RPV was generated, partially shown in Figures 3 and 4; it is discretized by a fully tetrahedral mesh containing about 20 million cells. The fluid physical properties remain the same as those of the experimental fluid calculated according to the temperature (70 °C) and pressure (1 bar) based on the data from the International Association for the Properties of Water and Steam (IAPWS-97) (IAPWS, 2007).

The distribution of the normalized flowrate at the core inlet obtained by the simulation is presented in Figure 5. Compared to the experimental results, the general trend of the flowrate distribution is captured well by the numerical simulation. Quantitatively, by defining the point-wise relative error of the flowrate distribution prediction as Eq. 4, the averaged relative error of all the available data was about 3.0%, with the maximal relative error 9.1% and the relative error standard deviation 2.1%. The current numerical framework can, to a certain degree, ensure the accuracy of CFD predictions for the three-dimensional flow field in the RPV and the flowrate distribution at the core inlet.

$$e_i = \left| \eta_i^{CFD} - \eta_i^{Exp} \right| \Big/ \eta_i^{Exp}. \tag{4}$$

It is known that the flow patterns of the coolant vary in different regions in the RPV, so it is almost impossible to precisely predict the flow by the CFD simulation with any standard turbulence model. Since the target of the CFD simulation is to obtain the precise distribution of the normalized flowrate at the core inlet based on the experimental results, some methods of coupling with data-driven machine learning technology can be utilized to optimize the turbulent model coefficient and improve the accuracy of the flowrate distribution prediction. For instance, data assimilation (DA) is a useful tool for coupling experimental measurements and numerical simulation so that the uncertainty of CFD simulations can be reduced (Kato and Obayashi, 2012). The assimilation algorithms range from Bayesian inference, ensemble Karman filter (EnKF) to adjoint formulation. For the steady-state flow simulation in the present study, we suggest applying DA for turbulence model coefficient calibration according to the point-wise relative error of the flowrate distribution prediction. It is believed that, with such a physically informed machine learning method, the predictive results with the calibrated model should be consistent with the essential physics.
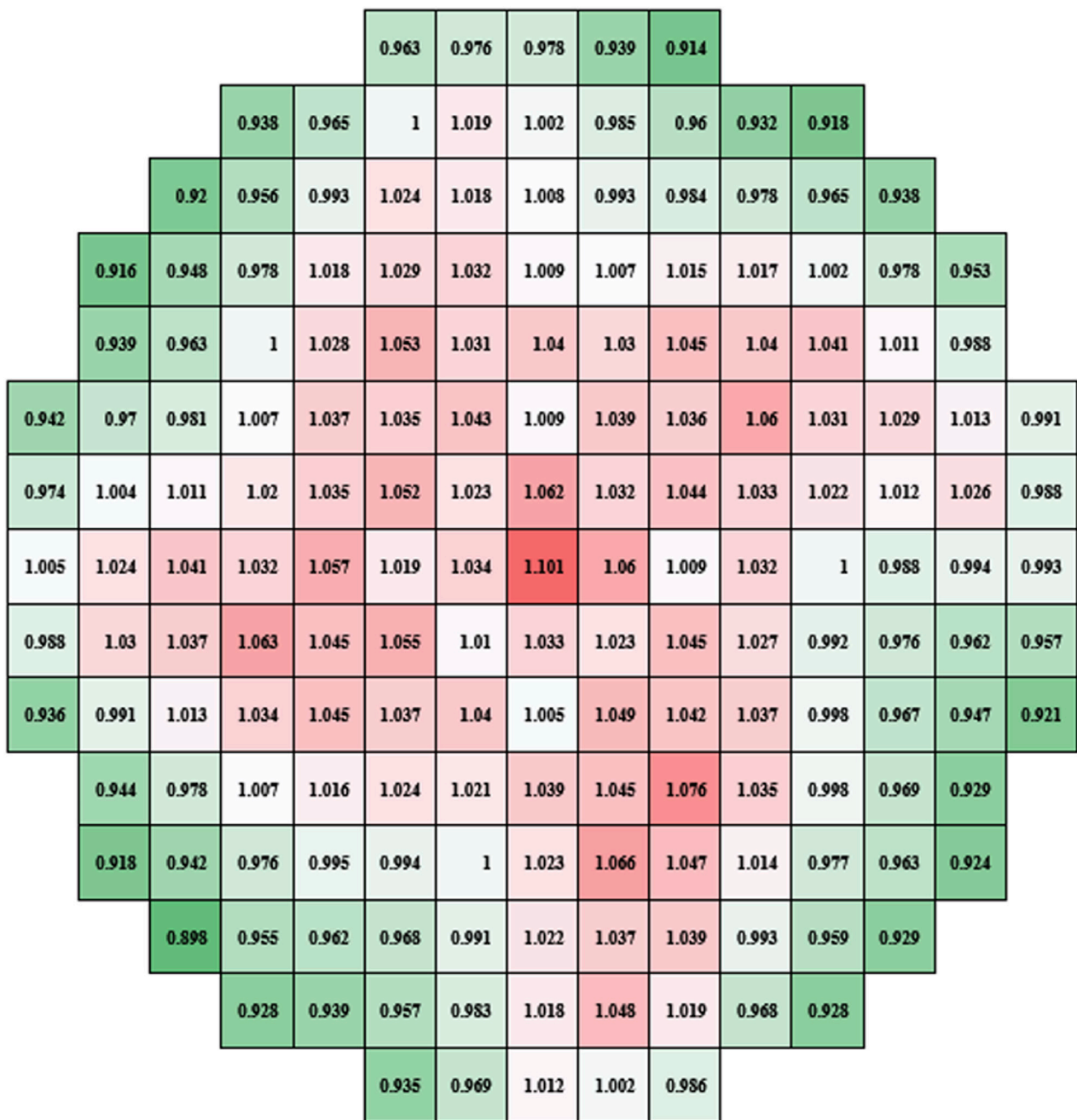
FIGURE 7
Distribution of the normalized flowrate at the core inlet of the Hualong One simulation.

3.2 Simulation results for Hualong One

The present Hualong One RPV shares overall structural similarities with the CNP1000 RPV while many local components, especially in the LP, have been optimized. In order to obtain the flowrate distribution at the core inlet under normal operation conditions in the Hualong One reactor, the validated CFD method with the standard turbulence model in the previous section was applied.

Figure 6 shows the velocity vector profiles in the LP. It can be observed that the local components in the LP exert strong effects on the coolant mixing by creating small eddies when the coolant passes by. Through the lower core plate which acts as a flow straightener, the coolant enters the core with the velocity remaining mostly in a vertical direction.

The normalized flowrate distribution predicted by the CFD simulation is shown in Figure 7. The distribution at the core inlet in Hualong One shows a shape similar to that in CNP1000. The distribution is also homogenous: the highest normalized flowrate (1.10) is at the
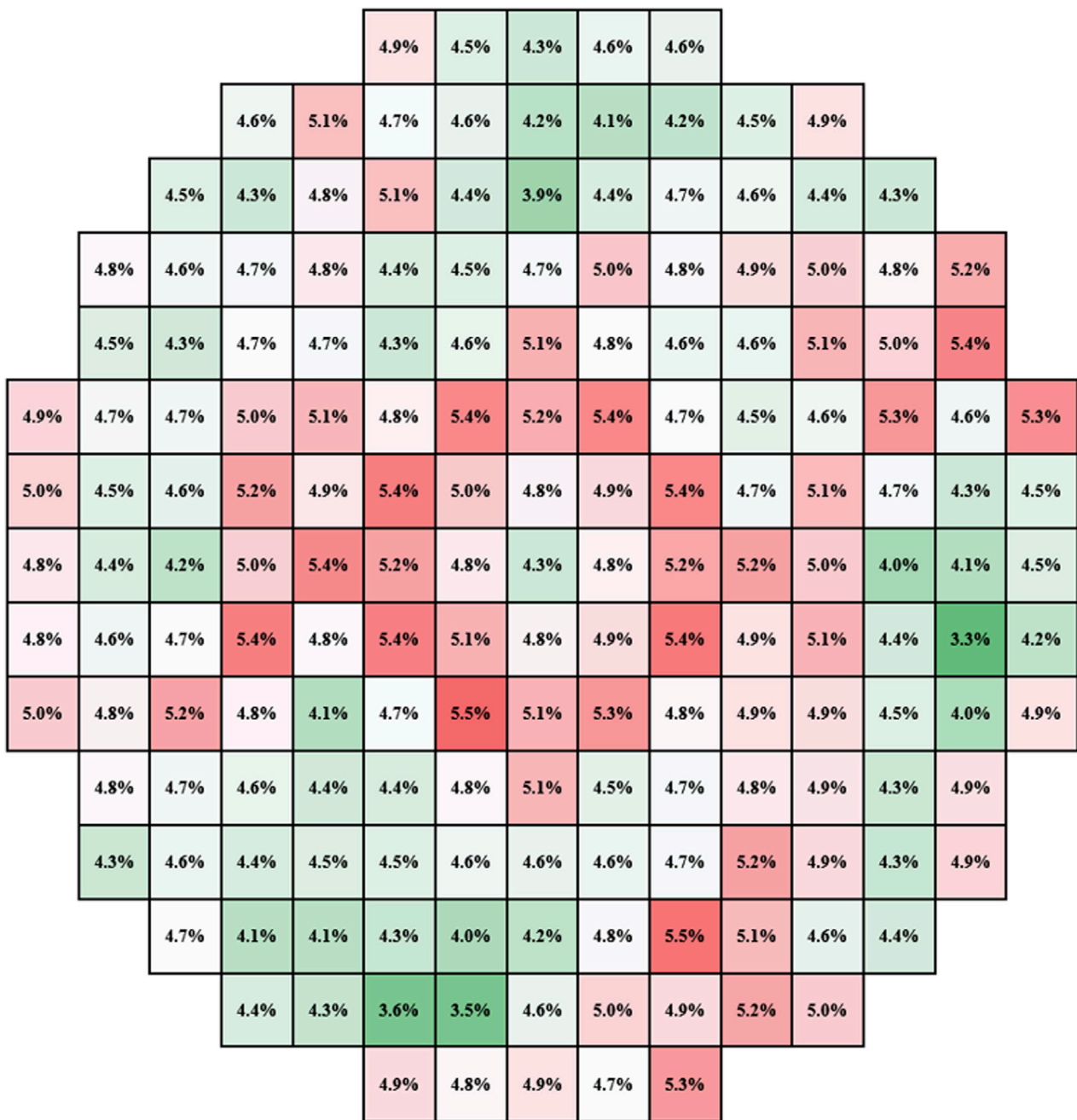
FIGURE 8
Distribution of the turbulent intensity at the core inlet of the Hualong One simulation.

center of the core inlet and the lowest normalized flowrate (0.90) is in the corner fuel assemblies. The average flowrate of the 5 × 5 assembly bundle in the middle region is about 1.04, and the maximal relative flowrate difference of the neighboring assemblies is lower than 5.5%.

More detailed information about the flow field in the RPV can be extracted from the numerical results. For instance, the average turbulent kinetic energy can be computed for each assembly, and the ratio between the average turbulent kinetic energy and the average velocity can be used to represent the turbulent intensity at the inlet of each fuel assembly. The definition of turbulent intensity is shown as Eq. 5:

$$I_i = \sqrt{\frac{2k_i}{3}} \bigg/ \frac{Q_i}{S}, \tag{5}$$

where k_i and Q_i are the average turbulent kinetic energy and the flowrate at the inlet of the i-th fuel assembly, respectively, and S is the area of the cross section in one fuel assembly. The distribution of the turbulent intensity at the core inlet from the Hualong One simulation is presented in Figure 8. The lower intensity region is at the middle and side of the core, while the higher intensity region is mainly located in the internal fuel assemblies.

4 Conclusion

The current study presents the CFD simulation result for a three-dimensional flow field in the Hualong One NPP RPV. The numerical framework is validated against the CNP1000 integral hydraulic experiments in a scaled test facility. The distribution of the normalized flowrate at the core inlet from the Hualong One simulation shows that, at the core inlet, the coolant flowrate is nearly homogenous and the turbulent intensity is acceptably low for each fuel assembly. This can provide essential information for the reactor core thermal–hydraulic design and fuel assembly mechanical assessment.

Data availability statement

The raw data supporting the conclusion of this article will be made available by the authors, without undue reservation.

Author contributions

WZ: writing–original draft and writing–review and editing. LS: conceptualization, supervision, and writing–review and editing. DS: validation and writing–review and editing. YL: methodology, validation, and writing–original draft. QZ: methodology, software, and writing–review and editing.

Conflict of interest

The authors declare that the research was conducted in the absence of any commercial or financial relationships that could be construed as a potential conflict of interest.

Publisher's note

All claims expressed in this article are solely those of the authors and do not necessarily represent those of their affiliated organizations or those of the publisher, the editors, and the reviewers. Any product that may be evaluated in this article, or claim that may be made by its manufacturer, is not guaranteed or endorsed by the publisher.

References

Bieder, U., Fauchet, G., Bétin, S., Kolev, N., and Popov, D. (2007). Simulation of mixing effects in a VVER-1000 reactor. *Nucl. Engeering Des.* 237, 1718–1728. doi:10.1016/j.nucengdes.2007.02.015

Ferziger, J. H., and Peric, M. (2001). *Computational methods for fluid Dynamics*. Springer.

Frepoli, C. (1996). Numerical simulation of the inlet plenum flow field for a LWR reactor pressure vessel. *Appl. Math. Model.* 253, 20. doi:10.1016/0307-904X(95)00153-B

Gango, P. (1997). Numerical boron mixing studies for Loviisa nuclear power plant. *Nucl. Engeering Des.* 177, 239–254. doi:10.1016/s0029-5493(97)00197-0

Gavrilas, M., and Kiger, K. (2000). *OECD/CSNI ISP Nr. 43 rapid boron-dilution transient tests for code verification*. Forschungszentrum Rossendorf, DE: NEA/CSNI/R, 22.

Glover, G. M. C., Höhne, T., Kliem, S., Rohde, U., Weiss, F. P., and Prasser, H. M. (2007). Hydrodynamic phenomena in the downcomer during flow rate transients in the primary circuit of a PWR. *Nucl. Engeering Des.* 237, 732–748. doi:10.1016/j.nucengdes.2006.08.010

Höhne, T., Kliem, S., Rohde, U., and Weiss, F.-P. (2007). Modeling of a buoyancy-driven flow experiment at the ROCOM test facility using the CFD-Code AFSYS CFX. *Kernkraftwerke Deutschl. Betriebsergebnisse* 52, 168–147.

Kato, H., and Obayashi, S. (2012). "Statistical approach for determining parameters of a turbulence model". In Proceding of the 15tg International Conference on Information Fusion.

Launder, B. E., and Sharma, B. I. (1974). Application of the energy-dissipation model of turbulence to the calculation of flow near a spinning disc. *Lett. Heat Mass Transf.* 1 (2), 131–137. doi:10.1016/0735-1933(74)90024-4

Lien, F. S., Chen, W. L., and Leschziner, M. (1996). "Low-Reynolds-number eddy-viscosity modelling based on non-linear stress-strain/vorticity relations," in *Engineering turbulence modelling and experiments* (Oxford: Elsevier), 91–100.

Menter, F. R., Kuntz, M., and Langtry, R. (2003). "Ten years of industrial experience with the SST turbulence model," in *4th Internal Symposium: turbulence, heat and mass transfer*.

Moukalled, F., Mangani, L., and Darwish, M. (2016). *The finite volume method in computational fluid Dynamics*. Springer.

Pope, S. B. (2000). *Turbulent flows*. Cambridge University Press.

IAPWS (2007). "Release on the IAPWS industrial formulation 1997 for the thermodynamic properties of water and steam," in *The international association for the properties of water and steam*.

Rohde, U., Höhne, T., Kliem, S., Hemstrom, B., Scheuerer, M., Toppila, T., et al. (2007). Fluid mixing and flow distribution in a primary circuit of a nuclear pressurized water reactor—validation of CFD codes. *Nucl. Engeering Des.* 15. doi:10.1016/j.nucengdes.2007.03.015

Rohde, U., Kliem, S., Höhne, T., Karlsson, R., Hemström, B., Lillington, J., et al. (2005). Fluid mixing and flow distribution in the reactor circuit, measurement data base. *Nucl. Engeering Des.* 235, 421–443. doi:10.1016/j.nucengdes.2004.08.045

Schaffrath, A., Fischer, K.-C., Hahm, T., and Wussow, S. (2007). Validation of the CFD code fluent by post-test calculation of a density-driven ROCOM experiment. *Nucl. Engeering Des.* 29. doi:10.1016/j.nucengdes.2007.02.029

Wilcox, D. C. (1993). *Turbulence modeling for CFD*. La Canada, CA: DCW Industries, Inc.

Zonglan, W., Bojan, N., Puragliesi, R., and Fogliatto, E. (2022). Assessment of turbulent heat flux models for URANS simulations of turbulent buoyant flows in ROCOM tests. *Nucl. Engeering Technol.* 54, 4359–4372. doi:10.1016/j.net.2022.07.009